Global Inorganic Source of Atmospheric Bromine

ARTICLE *in* THE JOURNAL OF PHYSICAL CHEMISTRY A · OCTOBER 2007

Impact Factor: 2.69 · DOI: 10.1021/jp074903r · Source: PubMed

THE JOURNAL OF PHYSICAL CHEMISTRY A LETTERS

2007, *111,* 8749−8752
Published on Web 08/22/2007

Global Inorganic Source of Atmospheric Bromine

S. Enami, C. D. Vecitis, J. Cheng, M. R. Hoffmann, and A. J. Colussi*

W. M. Keck Laboratories, California Institute of Technology, Pasadena, California 91125

Received: June 22, 2007; In Final Form: July 20, 2007

A few bromine molecules per trillion (ppt) causes the complete destruction of ozone in the lower troposphere during polar spring and about half of the losses associated with the "ozone hole" in the stratosphere. Recent field and aerial measurements of the proxy BrO in the free troposphere suggest an even more pervasive global role for bromine. Models, which quantify ozone trends by assuming atmospheric inorganic bromine (Br_y) stems exclusively from long-lived bromoalkane gases, significantly underpredict BrO measurements. This discrepancy effectively implies a ubiquitous tropospheric background level of ∼4 ppt Br_y of unknown origin. Here, we report that I^- efficiently catalyzes the oxidation of Br^- and Cl^- in aqueous nanodroplets exposed to ozone, the everpresent atmospheric oxidizer, under conditions resembling those encountered in marine aerosols. Br^- and Cl^-, which are rather unreactive toward O_3 and were previously deemed unlikely direct precursors of atmospheric halogens, are readily converted into IBr_2^- and ICl_2^- en route to Br_2(g) and Cl_2(g) in the presence of I^-. Fine sea salt aerosol particles, which are predictably and demonstrably enriched in I^- and Br^-, are thus expected to globally release photoactive halogen compounds into the atmosphere, even in the absence of sunlight.

Bromine critically affects atmospheric ozone at all altitudes, playing a crucial role in the ozone depletion events (ODEs) observed in the polar lower troposphere during early spring.[1−3] Despite its lower abundance, bromine is up to 45−70 times more efficient than chlorine as a catalyst of stratospheric ozone depletion.[4] The mechanism of atmospheric bromine production from its primary seawater bromide source is, however, not fully understood.[5] It has been generally assumed that gaseous inorganic bromine (Br_y) is actually released in the stratosphere by the short wavelength photolysis of long-lived source gases, such as biogenic methyl bromide and anthropogenic halons.[6] However, recent field, balloon, and satellite BrO measurements, which are broadly consistent with each other, significantly exceed model predictions based on those assumptions.[7−9] The implication is that some Br_y is directly delivered in the free troposphere, likely carried by sea salt aerosol itself.[8,10−12] Marine aerosols, which consist of fine particles that remain suspended long enough to undergo chemical processing, appear to be ideal vehicles for halogen activation. On the other hand, ODEs require the presence of appreciable levels (≳10 ppt) of rapidly photolyzable Br_2(g) in the boundary layer at the end of the polar winter night.[13−15] In this case, halogen activation may partially occur on the surface of the frozen sea. Since ODEs are also observed under pristine Antarctic conditions, the conversion of marine Br^- into Br_2(g) should involve natural oxidants that persist in the dark, such as O_3. Notably, the inertness of Br^- and Cl^- toward O_3 is somehow circumvented in sea salt.[16] The fact that more Br_2(g) is emitted from sea salt than from pure NaBr exposed to O_3(g) implies that Br^- oxidation is catalyzed by minor, unidentified components.[17] These observations suggest that the documented enrichment of specific seawater anions such as Br^- and I^- in fine marine aerosol particles could be an essential feature of the mechanism of halogen activation.[18−20]

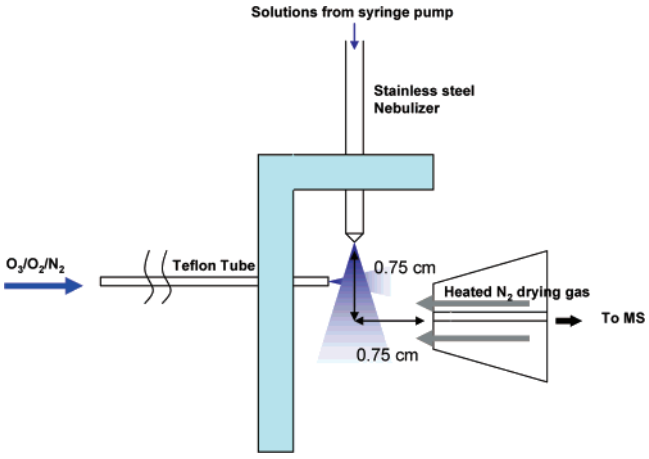

Figure 1. Schematic diagram of the spraying chamber, O_3(g) injection, and mass spectrometer sampling inlet.

We investigated this possibility in laboratory experiments in which the aerial interface of aqueous halide droplets sprayed into dilute O_3(g) is monitored via electrospray mass spectrometry (ESMS) of the evaporated anions (Figure 1). Further details are provided as Supporting Information (SI). Relative anion populations, f_i, at the interface of droplets produced from equimolar solutions were recently shown to increase exponentially with ionic radius, r_i; that is, $f_i \propto \exp(\beta r_i)$, $f_{I^-}/f_{Br^-} = 5.2$, $f_{Br^-}/f_{Cl^-} = 3.4$.[21] This correlation reveals that anion fractionation at the air/water interface is simply another manifestation of the Hofmeister

* To whom correspondence should be addressed. E-mail: ajcoluss@caltech.edu.

10.1021/jp074903r CCC: $37.00

effects generally observed at aqueous interfaces with less polarizable media.[22]

Small drops are usually charged, even when produced by fragmentation of electrically neutral liquids, due to statistical fluctuations that scale with (drop size)$^{-1/2}$.[23] For example, submicrometer marine aerosol drops are, on average, negatively charged.[24] Water evaporation, as regulated by ambient relative humidity, eventually shrinks the suspended drops, thereby increasing electrostatic repulsion among excess surface charges. Coulomb explosions ensue in which drops shed interfacial charge and mass into smaller droplets.[25] These events, when replicated by progeny droplets both in the marine aerosol and in our spraying chamber, ultimately generate small particles that are multiplicatively enriched (i.e., net enrichment $\propto (f_i)^m$, where m is the number of successive Coulomb explosions) in Br^- and I^-. This mechanism provides a physicochemical, that is, abiotic,[1,26] explanation for anion enrichment in aerosol particles, as well as for its inverse dependence on particle size and statistical variations among individual particles of similar size.[19] Since smaller particles draw mass and charge from larger units, it follows that Br^- is enriched in submicrometer particles but depleted in larger specimens.[2] In this context, the observation that $[Na^+]$ in polar snow decays exponentially with distance from the coast, as expected from the settling of marine aerosol particles whereas $[Br^-]$ remains nearly constant is interpreted as evidence that the finer aerosol, which is transported farther inland, is exponentially enriched in Br^-.[27]

Figure 2a shows the extent of I^- oxidation in aqueous NaI microdroplets injected in O_3(g) gas mixtures at atmospheric pressure. The interfacial I^- concentration decreases by ~50% after exposure to $[O_3(g)] \simeq 100$ ppm for ≃1 ms, that is, I^- reacts with O_3 with an apparent pseudo-first-order rate constant, $k^I \sim 10^3\ s^{-1}$, that can be formally calculated from the reaction rate constant in bulk solution: $k^{II}(I^- + O_3)_{aq} = 1.2 \times 10^9\ M^{-1}\ s^{-1}$,[28] and $[O_3(aq)] \sim 1\ \mu M$ (from Henry's law constant $H = 0.01\ M\ atm^{-1}$ for O_3 in water at 298 K). However, I^- oxidation at air/microdroplet interfaces may generally proceed at rates R_{-I^-} given by $R_{-I^-} \propto [I^-]^n[O_3(g)]$. In this context, $0.5 \le n \le 1$ is an effective reaction order that encodes the competition between mass transfer and chemical reaction at the gas−liquid interface. The actual n value is obtained from the steady-state condition: $IF(I^-) - [I^-]\tau^{-1} - k_R[I^-]^n[O_3(g)] = 0$, where $IF(I^-)$ is the I^- inflow to the reaction zone, that is, the intersection between the droplets and the O_3(g) plumes in Figure 1. τ is the transit time through this zone, and k_R is the effective reaction rate constant.[29] Since $IF(I^-) - [I^-]_0\tau^{-1} = 0$ at $[O_3(g)] = 0$, a plot of $([I^-]_0 - [I^-])/[I^-]^n$ vs $[O_3(g)]$ should be linear. The data of Figure 2a are linearized provided that $\langle n \rangle = 0.67 \pm 0.03$ in the range $1 \le [NaI]/\mu M \le 30$ ($[I^-] = 0.5\ \mu M$ in seawater) (Figure 2b). We verified that $\langle n \rangle \to 1$ as $[I^-] \to 500\ \mu M$, as expected for a surface-specific gas−liquid reaction.[30,31] From these experiments, we estimate that it takes ~40 min to oxidize 50% of the iodide contained in microdroplets suspended in typical ~40 ppb (parts per billion) atmospheric O_3(g) concentrations. R_{-I^-} is independent of bulk pH in the range 4.0−7.0. The simultaneous detection of iodate, IO_3^- ($m/z = 175$) and triiodide, I_3^- ($m/z = 381$) as products of I^- oxidation by O_3 in this system implies that their putative precursor, the HOI intermediate formed in reaction 1,

$$I^- + O_3 + H^+ = HOI + O_2 \qquad (1)$$

also has a reactive half-life shorter than ~1 ms. This finding is, however, at odds with estimates based on bulk solution kinetic data and conditions. From $k^{II}(HOI + O_3)_{aq} = 3.6 \times 10^4\ M^{-1}\ s^{-1}$,[32] $k^{II}(HOI + I^- + H^+)_{aq} = 4.4 \times 10^{12}\ M^{-2}\ s^{-1}$,[33] $[O_3(aq)] \sim 1\ \mu M$, and $[I^-] \sim 10\ \mu M$, at pH ~ 7, we estimate HOI half-lives toward oxidation by O_3 ($t_{1/2} = 19$ s) and reaction with I^- ($t_{1/2} = 0.16$ s) that are significantly longer than 1 ms. As expected from Scheme 1, the $[IO_3^-]/[I_3^-]$ ratio is an increasing function of $[O_3(g)]$ (Figure 3). Relative interfacial anion concentrations were derived from ESMS signal intensities, S, corrected by the response factors $[IO_3^-]/[I^-] = 0.80 \times S(IO_3^-)/S(I^-)$ and $[I_3^-]/[I^-] = 0.76 \times S(I_3^-)/S(I^-)$ determined under present experimental conditions. Note that the detected I_3^-, which is presumably involved in the fast equilibrium $I_2 + I^- \rightleftarrows I_3^-$ ($K_{eq} = 740\ M^{-1}$), must actually desorb from

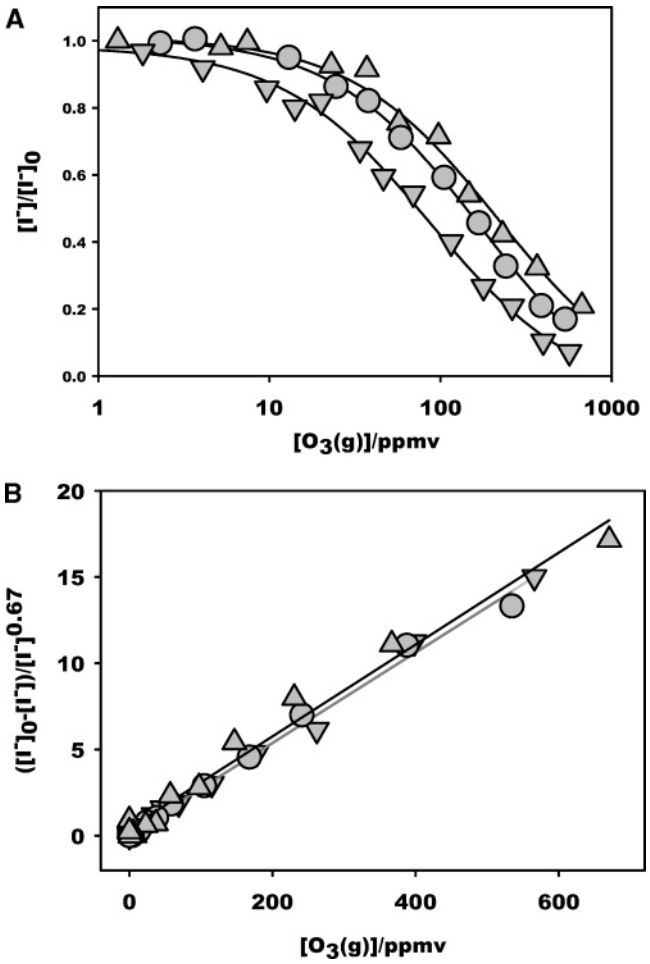

Figure 2. (a) Normalized interfacial iodide concentrations $[I^-]/[I^-]_0$ versus $[O_3(g)]$ (in 1 atm N_2) in ▼, 1 μM; ●, 10 μM; ▲, 30 μM NaI droplets. (b) Linearized plot of the data of part a. See text.

SCHEME 1

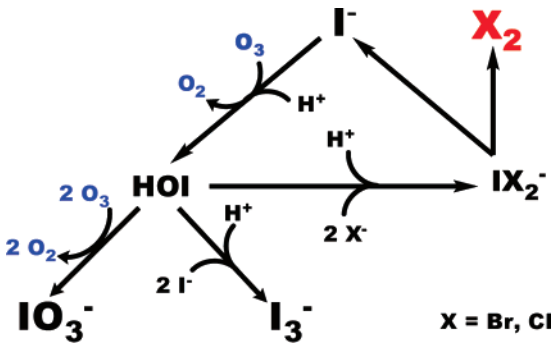

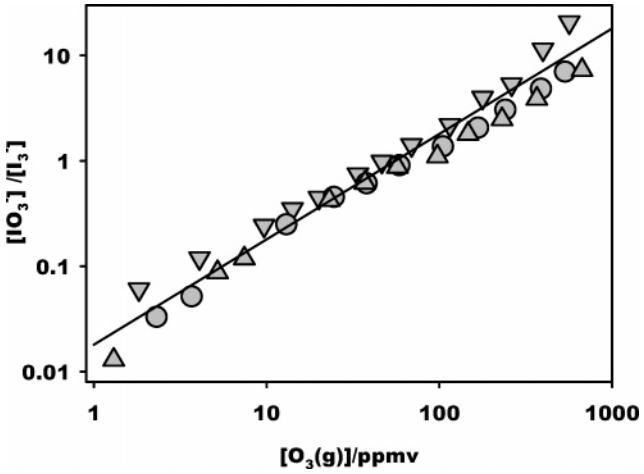

Figure 3. The $[IO_3^-]/[I_3^-]$ ratio as function of $[O_3(g)]$. ▼, 1 μM; ●, 10 μM; ▲, 30 μM NaI. The straight line corresponds to a linear $[IO_3^-]/[I_3^-]$ vs $[O_3(g)]$ dependence.

microdroplets in which $[I^-]$ necessarily exceeds the micromolar range. Thus, although I^- is oxidized to HOI immediately after the droplets enter the $O_3(g)$ plume, subsequent chemistry takes place in the increasingly concentrated aqueous media resulting from rapid solvent evaporation.[25] Similar conditions are expected to develop, albeit at a slower pace, in the marine aerosol.[34] IO_3^- and I_3^- yields calculated from interfacial I^- losses ($m/z = 127$) circumstantially exceed unity, revealing that interfacial layers are competitively replenished with I^- from the droplets core. It is apparent that the rates and mechanisms of chemical reactions at aerosol interfaces cannot be directly inferred from those in bulk solution.[35]

We confirmed that aqueous Br^- and Cl^- are inert toward O_3 under the present conditions, in line with reported rate constants $k^{II}(Br^- + O_3)_{aq} = 248\ M^{-1}\ s^{-1}$ [28] and $k^{II}(Cl^- + O_3)_{aq} = 0.1\ M^{-1}\ s^{-1}$, that are $\gtrsim 10^7$ times smaller than $k^{II}(I^- + O_3)_{aq}$ in bulk solution. However, ozonation experiments performed on (NaI + NaBr) and (NaI + NaCl) solutions readily yield the trihalide anions IBr_2^- and ICl_2^- (Figure 4A and B). IBr_2^- and ICl_2^- production rates increase with $[O_3(g)]$ (Figure 5) whereas Br^- inhibits I^- depletion and depresses IO_3^- and I_3^- formation (Figure 6). IBr_2^- and ICl_2^- are, therefore, the products of Br^- and Cl^- oxidation by I-containing intermediates, such as HOI or the primary adduct $I{-}OOO^-$, that are considerably more reactive than O_3. Since rate constants for the reactions of halide anions with HOI are commensurate ($I^- \sim Br^- \sim 10\ Cl^-$),[36] the huge selectivity of the stronger oxidizer O_3 for I^- versus Br^-/Cl^- is counterintuitive. Note that spin conservation requires the formation of excited $O_2(^1\Delta_g)$ in reaction 1 or its Br^-/Cl^- analogues. This restriction is more likely to be lifted by I^- than by Br^- or Cl^- via heavy atom enhancement of crossing rates into the triplet manifold that leads to ground state $O_2(^3\Sigma_g)$.[37] By mitigating spin conservation constraints, reaction 1 becomes the gateway to the I^--catalyzed production of Br_2 (and Cl_2) from sea salt (Scheme 1). The efficiency of this cycle (i.e., the $[Br_2]/[IO_3^-]$ ratio) is expected to be a direct function of $[Br^-]/[O_3]$ at the droplets' interface. Since Cl^- will always be present in large excess ($[Cl^-]/[Br^-]/[I^-] = 1.1 \times 10^6/1680/1$ in seawater) sea salt particles exposed to $O_3(g)$ will generate IBr_2^- and ICl_2^- rather than I_3^-, depending on actual interfacial halide and $O_3(g)$ concentrations; and some Br^- will remain even after extensive atmospheric processing. Scheme 1 provides a plausible mechanism for buffering the $[IO_3^-]/[I^-]$ ratio.[38]

Present experiments and analysis strongly suggest that I^- is the "minor component" that enhances O_3 uptake and concomitant Br_2 formation in sea salt.[17] The catalytic cycle of Scheme 1 qualifies as the previously unidentified dark process that liberates $Br_2(g)$ from sea salt into the boundary layer during the polar winter night[15] and primes the sudden destruction of O_3 at sunrise.[1] The proposed mechanism of marine halide oxidation operates incessantly over the oceans worldwide, rather than just around coastal regions, at rates that may be locally modulated by wind speed, relative humidity and atmospheric ozone concentration, but will not exhibit obvious latitudinal gradients or secular trends.[8] The fast halogen activation rates demonstrated by our experiments may generally exceed aerosol transport rates. Summing up, fine marine aerosols are expected to be naturally enriched in I^- and Br^- and therefore globally release gaseous halogen species into the atmosphere, even in the absence of sunlight.

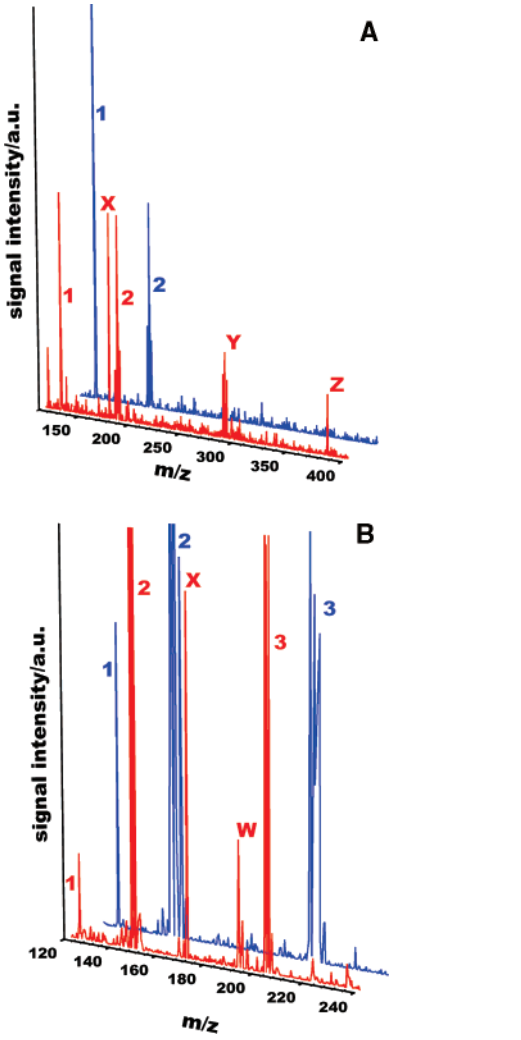

Figure 4. (a) Reaction products of bromide reaction with $O_3(g)$ in the presence of iodide. Negative ion mass spectra of aqueous (10 μM NaI + 100 μM NaBr) droplets. Blue trace: mass spectrum in 1 atm N_2. Peak 1: $m/z = 127$ (I^-). Peak group 2: $m/z = 181$, 183, and 185 ($NaBr_2^-$). Red trace: mass spectrum in [840 ppm $O_3(g)$ in 1 atm N_2] gas mixtures. New peaks correspond to reaction products. Peak X: $m/z = 175$ (IO_3^-). Peak group Y: $m/z = 285$ ($I^{79}Br^{79}Br^-$), 287 ($I^{79}Br^{81}Br^-$), 289 ($I^{81}Br^{81}Br^-$). Peak Z: $m/z = 381$ (I_3^-). (b) Reaction products of chloride reaction with $O_3(g)$ in the presence of iodide. Negative ion mass spectra of aqueous (10 μM NaI + 10 mM NaCl) droplets. Blue trace: mass spectrum in 1 atm N_2. Peak 1: $m/z = 127$ (I^-). Peak group 2: $m/z = 151$, 153, 155, and 157 ($Na_2Cl_3^-$). Peak group 3: $m/z = 209{-}217$ ($Na_3Cl_4^-$). Red trace: mass spectrum in [690 ppm $O_3(g)$ in 1 atm N_2] gas mixtures. New peaks correspond to reaction products. Peak X: $m/z = 175$ (IO_3^-). Peak group W: $m/z = 197$ ($I^{35}Cl^{35}Cl^-$), 199 ($I^{35}Cl^{37}Cl^-$), 201 ($I^{37}Cl^{37}Cl^-$).

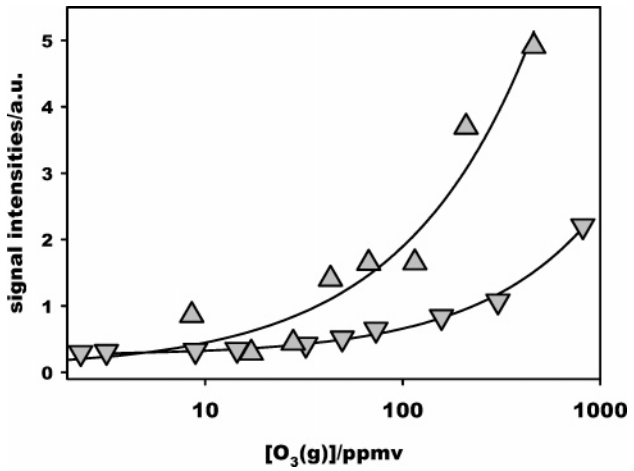

Figure 5. Reaction products of bromide and chloride reactions with $O_3(g)$ in the presence of iodide as a function of $[O_3(g)]$ (in 1 atm N_2). ▲: $m/z = 287$ ($I^{79}Br^{81}Br^-$) from ([NaI] = 10 μM + [NaBr] = 5 mM) droplets. ▼: $m/z = 197$ ($I^{35}Cl^{35}Cl^-$) from (10 μM NaI + 10 mM NaCl) droplets. Note that the apparently nonvanishing intercepts result from the logarithmic abscissa scale.

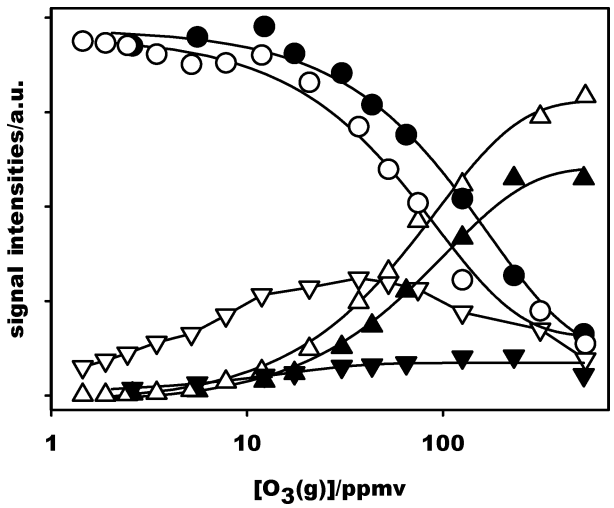

Figure 6. Reactant and products of iodide oxidation by $O_3(g)$ as a function of $[O_3(g)]$ (in 1 atm N_2) in the presence of NaBr. Open symbols: experiments in 10 μM NaI. Filled symbols: experiments in (10 μM NaI + 1 mM NaBr). ○, $m/z = 127$ (I^-); △, $m/z = 175$ (IO_3^-); ▽, $m/z = 381$ (I_3^-).

Acknowledgment. This project was financially supported by the National Science Foundation (ATM-0534990). S.E. is grateful to Prof. M. Kawasaki (Kyoto University), Prof. Y. Matsumi (Nagoya University). and the JSPS Research Fellowship for Young Scientists.

Supporting Information Available: Experimental details, further tests, and results. This material is available free of charge via the Internet at http://pubs.acs.org.

References and Notes

(1) Barrie, L. A.; Bottenheim, J. W.; Schnell, R. C.; Crutzen, P. J.; Rasmussen, R. A. *Nature* **1988**, *334*, 138.

(2) Sander, R.; Keene, W. C.; Pszenny, A. A. P.; Arimoto, R.; Ayers, G. P.; Baboukas, E.; Cainey, J. M.; Crutzen, P. J.; Duce, R. A.; Honninger, G.; Huebert, B. J.; Maenhaut, W.; Mihalopoulos, N.; Turekian, V. C.; Van Dingenen, R. *Atmos. Chem. Phys.* **2003**, 1301.

(3) Yang, X.; Cox, R. A.; Warwick, N. J.; Pyle, J. A.; Carver, G. D.; O'Connor, F. M.; Savage, N. H. *J. Geophys. Res.* **2005**, *110*, D23311.

(4) Sinnhuber, B. M.; Sheode, N.; Sinnhuber, M.; Chipperfield, M. P. *Atmos. Chem. Phys. Discuss.* **2006**, 6497.

(5) Simpson, W. R.; Von Glasow, R.; Riedel, K.; Anderson, P.; Ariya, P.; Bottenheim, J. W.; Burrows, J.; Carpenter, L.; Friess, U.; Goodsite, M. E.; Heard, D.; Hutterli, M.; Jacobi, H. W.; Kaleschke, L.; Neff, B.; Plane, J.; Platt, U.; Richter, A.; Roscoe, H.; Sander, R.; Shepson, P. B.; Sodeau, J.; Steffen, A.; Wagner, T.; Wolff, E. *Atmos. Chem. Phys. Discuss.* **2007**, *7*, 4285.

(6) World Metereological Organization (WMO), Global Ozone Research and Monitoring Project; In *Scientific Assessment of Ozone Depletion: 2002*, Report No. 47; Geneva: 2003.

(7) Sioris, C. E.; Kovalenko, L. J.; McLinden, C. A.; Salawitch, R. J.; Van Roozendael, M.; Goutail, F.; Dorf, M.; Pfeilsticker, K.; Chance, K.; von Savigny, C.; Liu, X.; Kurosu, T. P.; Pommereau, J. P.; Bosch, H.; Frerick, J. *J. Geophys. Res.* **2006**, *111*, D14301.

(8) Dorf, M.; Butler, J. H.; Butz, A.; Camy-Peyret, C.; Chipperfield, M. P.; Kritten, L.; Montzka, S. A.; Simmes, B.; Weidner, F.; Pfeilsticker, K. *Geophys. Res. Lett.* **2006**, *33*, L24803.

(9) Schofield, R.; Johnston, P. V.; Thomas, A.; Kreher, K.; Connor, B. J.; Wood, S.; Shooter, D.; Chipperfield, M. P.; Richter, A.; von Glasow, R.; Rodgers, D. C. *J. Geophys. Res.* **2006**, *111*, D22310.

(10) Salawitch, R. J. *Nature* **2006**, *439*, 275.

(11) Salawitch, R. J.; Weisenstein, D. K.; Kovalenko, L. J.; Sioris, C. E.; Wennberg, P. O.; Chance, K.; Ko, M. K. W.; McLinden, C. A. *Geophys. Res. Lett.* **2005**, *32*, L05811.

(12) von Glasow, R.; von Kuhlmann, R.; Lawrence, M. G.; Platt, U.; Crutzen, P. J. *Atmos. Chem. Phys.* **2004**, *4*, 2481.

(13) Li, S. M.; Yokouchi, Y.; Barrie, L. A.; Muthuramu, K.; Shepson, P. B.; Bottenheim, J. W.; Sturges, W. T.; Landsberger, S. *J. Geophys. Res.* **1994**, *99*, 25415.

(14) Foster, K. L.; Plastridge, R. A.; Bottenheim, J. W.; Shepson, P. B.; Finlayson-Pitts, B. J.; Spicer, C. W. *Science* **2001**, *291*, 471.

(15) Hara, K.; Osada, K.; Matsunaga, K.; Iwasaka, Y.; Shibata, T.; Furuya, K. *J. Geophys. Res.* **2002**, *107*, D4361.

(16) Finlayson-Pitts, B. J. *Chem. Rev.* **2003**, *103*, 4801.

(17) Mochida, M.; Hirokawa, J.; Akimoto, H. *Geophys. Res. Lett.* **2000**, *27*, 2629.

(18) Lewis, E. R.; Schwartz, S. E. *Sea Salt Aerosol Production: Mechanisms, Methods, Measurements and Models—A Critical Review*; American Geophysical Union: Washington, DC, 2004; Vol. Geophysical Monograph 152.

(19) Murphy, D. M.; Thomson, D. S.; Middlebrook, A. M. *Geophys. Res. Lett.* **1997**, *24*, 3197.

(20) Murphy, D. M.; Cziczo, D. J.; Froyd, K. D.; Hudson, P. K.; Matthew, B. M.; Middlebrook, A. M.; Peltier, R. E.; Sullivan, A.; Thompson, D. S.; Weber, R. J. *J. Geophys. Res.* **2006**, *111*, D23S32.

(21) Cheng, J.; Vecitis, C.; Hoffmann, M. R.; Colussi, A. J. *J. Phys. Chem. B* **2006**, *110*, 25598.

(22) Pegram, L. M.; Record, M. T. *J. Phys. Chem. B* **2007**, *111*, 5411.

(23) Dodd, E. E. *J. Appl. Phys.* **1953**, *24*, 73.

(24) Reiter, R. *J. Geophys. Res.* **1994**, *99*, 10807.

(25) Kebarle, P. *J. Mass Spectrom.* **2000**, *35*, 804.

(26) Carpenter, L. J.; Hopkins, J. R.; Jones, C. E.; Lewis, A. C.; Parthipan, R.; Wevill, D. J. *Environ. Sci. Technol.* **2005**, *39*, 8812.

(27) Simpson, W. R.; Alvarez-Aviles, L.; Douglas, T. A.; Sturm, M.; Domine, F. *Geophys. Res. Lett.* **2005**, *32*, L04811.

(28) Liu, Q.; Schurter, L. M.; Muller, C. E.; Aloisio, S.; Francisco, J. S.; Margerum, D. W. *Inorg. Chem.* **2001**, *40*, 4436.

(29) Colussi, A. J.; Baghal-Vayjooee, M. H.; Benson, S. W. *J. Am. Chem. Soc.* **1978**, *100*, 3214.

(30) Davidovits, P.; Kolb, C. E.; Williams, L. R.; Jayne, J. T.; Worsnop, D. R. *Chem. Rev.* **2006**, *106*, 1323.

(31) Hanson, D. R. *J. Phys. Chem. B* **1997**, *101*, 4998.

(32) Bichsel, Y.; von Gunten, U. *Environ. Sci. Technol.* **1999**, *33*, 4040.

(33) Eigen, M.; Kustin, K. *J. Am. Chem. Soc.* **1962**, *84*, 1355.

(34) Gao, Y.; Chen, S. B.; Yu, L. E. *Atmos. Environ.* **2007**, *41*, 2019.

(35) Hunt, S. W.; Roeselova, M.; Wang, W.; Wingen, L. M.; Knipping, E. M.; Tobias, D. J.; Dabdub, D.; Finlayson-Pitts, B. J. *J. Phys. Chem. A* **2004**, *108*, 11559.

(36) Vogt, R.; Sander, R.; von Glasow, R.; Crutzen, P. J. *J. Atmos. Chem.* **1999**, *32*, 375.

(37) Muñoz, F.; Mvula, E.; Braslavsky, S. E.; von Sonntag, C. *J. Chem. Soc. Perkin Trans. 2* **2001**, 1109.

(38) Bruchert, W.; Helfrich, A.; Zinn, N.; Klimach, T.; Breckenheimer, M.; Chen, H.; Lai, S.; Hoffmann, T.; Bettmer, J. *Anal. Chem.* **2007**, *79*, 1714.